Calcium Signaling in Restricted Diffusion Spaces

Gary J. Kargacin
Department of Medical Physiology, University of Calgary, Calgary, Alberta T2N 4N1 Canada

ABSTRACT One- and two-dimensional models of Ca^{2+} diffusion and regulation were developed and used to study the magnitudes and the spatial and temporal characteristics of the Ca^{2+} transients that are likely to develop in smooth muscle cells in restricted diffusion spaces between the plasma membrane and intracellular organelles. Simulations with the models showed that high [Ca^{2+}] (on the order of several μM) can develop in such spaces and persist for 100–200 ms. These Ca^{2+} transients could: 1) facilitate the coupling of Ca^{2+} influx to intracellular Ca^{2+} release; 2) provide a mechanism for the regulation of stored Ca^{2+} that does not affect the contractile state of smooth muscle; 3) locally activate specific signal transduction pathways, before, or without activating other Ca^{2+} dependent pathways in the central cytoplasm of the cell. The latter possibility suggests that independent enzymatic processes in cells could be differentially regulated by the same intracellular second messenger.

INTRODUCTION

In previous work with one- and two-dimensional models of Ca^{2+} diffusion and regulation in smooth muscle cells, Kargacin and Fay (1991) suggested that high Ca^{2+} concentrations can develop near the plasma membrane in smooth muscle cells as a result of Ca^{2+} influx through membrane channels. High Ca^{2+} concentrations could also develop within the cytoplasm at sites where Ca^{2+} is released from the sarcoplasmic reticulum (SR). During the decline of a Ca^{2+} transient, localized regions of low [Ca^{2+}] were predicted to develop in cells where Ca^{2+} is taken back up into the SR and at sites on the plasma membrane where Ca^{2+} is pumped out of the cell. The fact that inhomogeneities in [Ca^{2+}] are likely to be present in smooth muscle cells during transient Ca^{2+} signals suggests that the spatial characteristics of a Ca^{2+} signal are important determinants of the response of the cell to the signal. For example, an external stimulus that invokes a substantial extracelluar influx of Ca^{2+} might activate enzymatic processes near the membrane that are not activated by an external stimulus that primarily invokes the release of Ca^{2+} from intracellular storage sites. Calcium influx into different regions of a cell could also influence cellular responses. Recent work by Bading et al. (1993) indicates that Ca^{2+} influx into neuronal cells, through different types of Ca^{2+} channels, results in the regulation of different signaling pathways. This finding can be explained if one assumes that each type of channel is localized to a specific region or regions of the plasma membrane and that the enzymes involved in each of the pathways are also confined spatially to submembrane regions near the channels.

Localized Ca^{2+} signaling would be especially important and prevalent in cells at locations where intracellular structures and organelles come into close contact with the surface membrane. At such sites, the physical presence of the structures would impede the free movement of Ca^{2+} into the central cytoplasm of the cell and, as a consequence, the Ca^{2+} concentrations developed in these restricted diffusion spaces would be higher and persist for longer times than those developed in regions where free diffusion could occur. The possibility that local high concentrations of Ca^{2+} or other ions can develop and influence cellular function in smooth muscle and other types of cells in regions where Ca^{2+} influx or release is directed into a narrow cytoplasmic space has been proposed by a number of investigators. It has been suggested that, when depleted of Ca^{2+}, the superficial SR in smooth muscle takes up a significant fraction of the Ca^{2+} moving into the cell from the extracelluar space and, thereby, reduces the amount of Ca^{2+} entering the cytoplasm (reviewed by van Breemen and Saida, 1989; Sturek et al., 1992). A number of laboratories (Benham and Bolton, 1986; Ohya et al., 1987; Hume and LeBlanc, 1989; Désilets et al., 1989; Stehno-Bittel and Sturek, 1992) have noted the spontaneous activation of Ca^{2+}-activated K^+ currents in smooth muscle, which appears to be the result of the spontaneous release of Ca^{2+} from intracellular storage sites. Benham and Bolton (1986) and Stehno-Bittel and Sturek (1992) have suggested that this release occurs in regions where the SR comes into close apposition to the plasma membrane. Local Ca^{2+} signaling in restricted diffusion spaces has also been postulated to occur in cardiac muscle (see Lederer et al., 1990; Leblanc and Hume, 1990) and neurons (see Smith and Augustine, 1988). The evidence for this type of signaling has been largely indirect, however, and the magnitudes and the spatial and temporal properties of the ionic signals in such spaces have not been explored experimentally.

Smooth muscle cells are organized in a manner that could promote and exploit local Ca^{2+} signaling. The membrane of the SR in smooth muscle can come into close apposition to the plasma membrane (see Devine et al., 1972; Somlyo, 1980; Gabella, 1983, Somlyo and Franzini-Armstrong, 1985). Where this occurs, the SR membrane can run parallel to the plasma membrane for distances of 1 μm or more (Devine et al., 1972; Gabella, 1983), and periodic structures

Received for publication 29 September 1993 and in final form 16 March 1994.

Address reprint requests to Dr. Gary J. Kargacin, Department of Medical Physiology, University of Calgary, 3330 Hospital Drive NW, Calgary, Alberta T2N 4N1 Canada. Tel.: 403-220-3873; Fax: 403-220-6848.

0006-3495/94/07/262/11 $2.00

that span the cytoplasmic space between the two membranes have been noted (Devine et al., 1972; Gabella, 1983; Somlyo and Franzini-Armstrong, 1985). The close contact and the presence of connecting structures between the SR and the surface membrane in smooth muscle cells suggests that these sites are specialized to promote the regulation of both cytoplasmic and stored Ca^{2+}. The spanning proteins could be directly involved in coupling excitation of the plasma membrane with release of stored intracellular Ca^{2+}, as are the foot proteins in cardiac and skeletal muscle (see Fleischer and Inui, 1989). Alternatively, the structures in smooth muscle might serve, primarily, to keep the membranes in close apposition. In this case, the Ca^{2+} channels and pumps on the plasma membrane could interact with Ca^{2+} release sites and pumps on the SR membrane as a result of the diffusion of Ca^{2+} or other substances through the narrow cytoplasmic space separating the two membranes.

To understand how local Ca^{2+} signals might develop in cells and influence specific signal transduction pathways, it is important to have theoretical knowledge of the likely magnitudes, time courses, and influences that can act on intracellular ionic signals, especially those that might arise in confined spaces. In the work reported here, the diffusion models described previously (Kargacin and Fay, 1991) were modified to explore specifically the properties of restricted diffusion spaces and their effects on Ca^{2+} signaling in smooth muscle cells. To provide a basic framework for understanding such signaling, the models were constructed without the imposition of any properties on the cell cytoplasm in the restricted spaces that were not similarly present in the rest of the cell.

Results of simulations with the models indicate that very high Ca^{2+} concentrations (on the order of several μM) are likely to develop in restricted diffusion spaces in smooth muscle cells. The high concentrations could persist for 100–200 ms after transient Ca^{2+} influx and/or release from the SR. These high Ca^{2+} concentrations could function to rapidly couple Ca^{2+} influx to Ca^{2+}-induced Ca^{2+} release from the SR and, thereby, compensate in part for the relatively low diffusion coefficient for Ca^{2+} in cells (see Allbritton et al., 1992). Local Ca^{2+} movement into a restricted space in smooth muscle cells could also provide a means by which the Ca^{2+} content of the SR could be regulated independently of changes in bulk cytoplasmic $[Ca^{2+}]$ and might be a means by which different enzymatic processes in the cell could be differentially controlled by the same second messenger. Use of the models to investigate the possibility of directly measuring the magnitude and time course of Ca^{2+} signals in restricted spaces suggested that such transients would be only poorly resolved by the fluorometric methods currently in common use.

MATERIALS AND METHODS

The basic components of the one- and two-dimensional models for Ca^{2+} diffusion and regulation in smooth muscle cells were described previously (Kargacin and Fay, 1991). These models were based, as much as possible, on available experimental results and incorporated equations describing Ca^{2+} influx and extrusion through the plasma membrane, Ca^{2+} uptake and release from the SR, and intracellular Ca^{2+} buffering. Only a general outline of the components included in the models will be presented here (for additional details about the equations and parameters used, the reader is referred to Kargacin and Fay, 1991). Note: in Eqs. 1–7 below, Ca denotes $[Ca^{2+}]_{free}$.

The diffusion equations for radial (r; Equation 1) and both radial and axial (r, z; Eq. 2) diffusion in the model smooth muscle cells are

$$\frac{\partial Ca}{\partial t} = \frac{1}{r}\frac{\partial}{\partial r}\left(rD\frac{\partial Ca}{\partial r}\right) + F(Ca, t, r) \tag{1}$$

and

$$\frac{\partial Ca}{\partial t} = \frac{1}{r}\frac{\partial}{\partial r}\left(rD\frac{\partial Ca}{\partial r}\right) + \frac{\partial}{\partial z}\left(D\frac{\partial Ca}{\partial z}\right) + F(Ca, t, r, z), \tag{2}$$

where $F(Ca, t, r)$ and $F(Ca, t, r, z)$ include the concentration, time, and position-dependent Ca^{2+} regulatory processes in the cell as described below (see also Fig. 1 in Kargacin and Fay, 1991). To improve the spatial resolution of the models over those described previously (Kargacin and Fay, 1991), the model cell (3-μm radius) was divided into 120 25-nm concentric annuli rather than the 30 (100 nm) annuli used previously. For the two-dimensional simulations, the model cell was divided into 30 (100 nm) or 60 (50 nm) annuli and 30–60 (100 nm) length elements. Movement of Ca^{2+} into and out of each spatial element in the models was computed using the explicit finite-difference formulation described by Crank (1975); see also Kargacin and Fay (1991). The smooth muscle plasma membrane Ca^{2+} pump was described by the Hill equation as

$$\frac{\Delta Ca}{\Delta t} = \frac{V_{max}(Ca)^n}{K_m^n + (Ca)^n} \tag{3}$$

with V_{max} the maximum velocity of the pump, K_m the $[Ca^{2+}]$ at half maximal velocity, and n the Hill coefficient. To balance the pump efflux in the resting cell so that no net removal of Ca^{2+} from the cytoplasm occurred, an inward Ca^{2+} leak was included in the simulations and was described by the equation

$$\frac{\Delta Ca}{\Delta t} = K_{leak}(Ca_{extracellular} - Ca_{cytoplasm}) \tag{4}$$

with K_{leak} adjusted so that the Ca^{2+} influx through the leak was equal to the the resting extrusion of Ca^{2+} through the plasma membrane. A similar pair of equations was used to describe the Ca^{2+} pump and a leak on the SR membrane when these elements were included in the model. In the latter case, $Ca_{extracellular}$ in Eq. 4 was replaced by the $[Ca^{2+}]$ in the SR (1.5 mM), and K_{leak} was adjusted to balance resting SR Ca^{2+} uptake. For the plasma membrane pump, V_{max} was 3.2×10^{-13} mol/cm^2 s, K_m was 200 nM, and n was 1 (see Kargacin and Fay, 1991; Lucchesi et al., 1988; Carafoli, 1987). For the SR pump, V_{max} was set at 3.5×10^{-12} mol/cm^2 s as described in Kargacin and Fay (1991). The other constants for the SR were K_m = 219 nM and n = 2 (see Kargacin et al., 1988). The extent to which Na^+/Ca^{2+} exchange contributes to Ca^{2+} regulation in smooth muscle cells is not well known (see Blaustein et al., 1991). To account for a possible contribution of the exchanger to Ca^{2+} extrusion, however, the velocity of the plasma membrane pump was doubled in the simulations with the model. This was based on the results of Cooney et al. (1991) (see also Kargacin and Fay, 1991), who suggest that Na^+/Ca^{2+} exchange contributes to Ca^{2+} extrusion to an extent equal to that of the plasma membrane pump. The Ca^{2+} buffers in the model cell were combined into a single fixed buffer distributed throughout the cell (total buffer concentration = 230 μM; see Bond et al., 1984; Allbritton et al., 1992). Buffering was described by the equation

$$\frac{\Delta Ca}{\Delta t} = -K_{on}([buffer]_{free})(Ca) + K_{off}[Ca]_{bound}, \tag{5}$$

with K_{on} and K_{off} the on and off rates of the buffer set at 10^8/M-s and 10^2/s, respectively (see Robertson et al., 1981; Kargacin and Fay, 1991). Ca^{2+} influx into the cell through the plasma membrane and into the cytoplasmic space from intracellular Ca^{2+} stores were described by equations

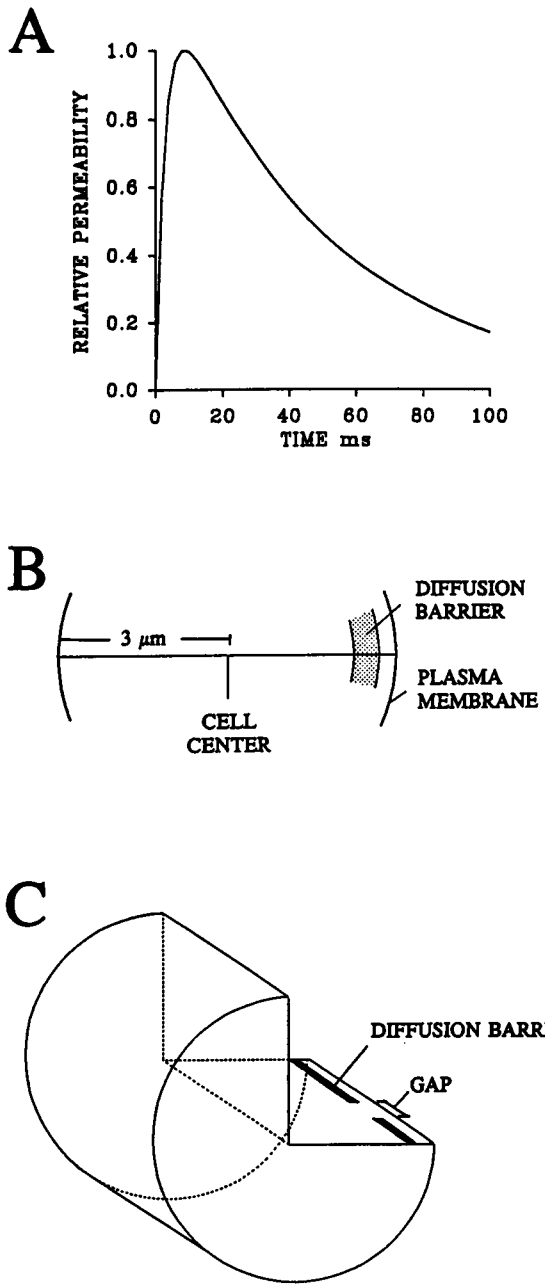

FIGURE 1 Time course of the Ca^{2+} permeability change and other elements incorporated into the one- and two-dimensional diffusion models. (*A*) Membrane permeability changes. Influx of Ca^{2+} through the plasma membrane and efflux from the SR were described by Eqs. 6 and 7. The time constants were adjusted as described in the text. (*B*) One-dimensional model. The cell diameter was 6 μm; extracelluar $[Ca^{2+}]$ was 1.5 mM; starting intracellular $[Ca^{2+}]_{free}$ was 150 nM. The shaded area represents a barrier to free diffusion that was imposed between the central cytoplasm of the model cell and that near the plasma membrane. The thickness of the barrier was 100 nm in all simulations. The distance between the barrier and the plasma membrane was varied in different simulations. When the barrier was assumed to be due to the presence of the SR near the plasma membrane, SR Ca^{2+} pumps, leak, and release sites were located either on the cytoplasmic side or the plasma membrane side of the barrier. The $[Ca^{2+}]_{free}$ inside the SR was assumed to be 1.5 mM. Components of the model describing Ca^{2+} influx, extrusion, and leakage through the plasma membrane and cytoplasmic Ca^{2+} buffering are discussed in the text. (*C*) Two-dimensional model. The Ca^{2+} regulatory components included in the two-dimensional model were the same as those used in the one-dimensional model, but both radial diffusion and diffusion along the cell length were modeled. The barrier to free diffusion (*dark bars*) in the two-dimensional model was not continuous in the length dimension but contained a gap (*space between dark bars*) through which free diffusion of Ca^{2+} into the central cytoplasm of the cell could occur.

of the form

$$\frac{\Delta Ca}{\Delta t} = K(Ca_{out} - Ca) \quad (6)$$

and

$$K = K_o(1 - \exp^{-t/t_{on}})(\exp^{-t/t_{off}}) \quad (7)$$

(see Cannell and Allen, 1984; Backx et al., 1989; Kargacin and Fay, 1991). The parameters t_{on} and t_{off} (3 and 50 ms, respectively) for plasma membrane influx were adjusted so that the time course of Ca^{2+} influx in the model cell matched the time course of the Ca^{2+} current measured by Becker et al. (1989) in voltage-clamped smooth muscle cells. The constant K_o was adjusted so that the average $[Ca^{2+}]_{free}$ reached in the model cell (without diffusion barriers present) matched the $[Ca^{2+}]_{free}$ (400–600 nM) measured experimentally in smooth muscle cells during Ca^{2+} transients. Adjustments to Eq. 7 for the two-dimensional model when small local currents (e.g., through single Ca^{2+} channels or clusters of channels) were modeled will be discussed later. The equation describing Ca^{2+} release from the SR had the same form and time constants as that used to describe influx through the plasma membrane except that, before release could start, the $[Ca^{2+}]_{free}$ at the SR membrane had to reach a preset level ([switch]). The time course of the SR and plasma membrane permeability changes is shown in Fig. 1 *A*. The equations describing Ca^{2+} influx through the plasma membrane, Ca^{2+} buffering, extrusion out of the cell, and the inward leak of Ca^{2+} through the plasma membrane were included in all simulations. Uptake and release of Ca^{2+} by the SR was only included in simulations in which these processes were studied. The positions of the SR uptake and release sites in the model cell were varied in different simulations.

In addition to the elements described above, the models were constructed to include a diffusion barrier (a region with a lower diffusion coefficient) near the surface membrane of the cell (Fig. 1, *B* and *C*). Diffusion through the barrier region was hindered by the lower diffusion coefficient and, as a result, a restricted diffusion space was created between the surface membrane and the barrier. The boundaries on either side of the barrier were treated as described by Crank (1975) for diffusion through composite media. The thickness of the cytoplasmic space between the barrier and the surface membrane of the model cell was varied in different simulations. Although it was possible in the model to prevent completely the movement of Ca^{2+} into the central cytoplasmic space behind the barrier by setting the diffusion coefficient through the barrier region equal to 0, it was more realistic to allow some Ca^{2+} to reach the central cytoplasmic space to account for Ca^{2+} movement along pathways that circumvented the barrier itself (i.e., pathways that involved the length and angle dimensions of the cell that were not modeled). For an impenetrable barrier of thickness b and length $2 \times l$, using the equation $r^2 = 2Dt$ to express the mean-square displacement of an ion diffusing through a medium with a diffusion coefficient D (see, for example, Hille, 1992), it can be seen that the amount of time (t) required for Ca^{2+} to move around the barrier (from the center of one side to the center of the other side; path length = $2l + b$) is equal to the amount of time required for Ca^{2+} to diffuse directly through the barrier region (path length = b) with a diffusion coefficient of $D_t = Db^2/(2l + b)^2$. For the simulations with the one-dimensional model described here, it was assumed that a typical intracellular barrier was 100 nm in thickness and extended parallel to the plasma membrane 100 nm in the length and angular directions beyond the site of Ca^{2+} influx. This assumption is consistent with the dimensions of the superficial SR in smooth muscle cells (see, for example, Gabella, 1983; Somlyo, 1980). To approximate this case, the diffusion coefficient through the barrier region in the model cell was set, therefore, at 0.1 × the coefficient in the rest of the cell.

The two-dimensional model (Fig. 1 *C*) was constructed with the same basic parameters as the one-dimensional model and permitted Ca^{2+}

movement to be studied simultaneously in both the radial direction and along the length of the cell. In the two-dimensional model, the diffusion barrier was not necessarily continuous along the cell length but could be interrupted by one or more gaps through which free diffusion into the bulk of the cytoplasm could occur. As was the case with the one-dimensional model, some diffusion through the barrier region was also allowed to occur to account for the movement of Ca^{2+} into the central cytoplasm through pathways involving the angular dimension. With the two-dimensional model, it was thus possible to look at restricted spaces in more global settings because movement through both restricted-diffusion regions and free-diffusion regions could be examined at the same time.

A Fortran program written by the author incorporating Eqs. 3–7 into the explicit finite differences formulae described by Crank (1975) (see also Kargacin and Fay, 1991) was used to obtain numerical solutions to Eqs. 1 and 2. The simulations were run on a 386 personal computer.

RESULTS AND DISCUSSION

Diffusion without a barrier

In previous work (Kargacin and Fay, 1991), an intracellular diffusion coefficient of 4×10^{-6} cm^2/s (based on estimates of the space not occupied by structures in electron micrographs of smooth muscle cells) was used to describe the movement of Ca^{2+} through the cytoplasm of the model cell. This number is approximately one-half the value of the diffusion coefficient for Ca^{2+} in water (7×10^{-6} cm^2/s; see Kushmerick and Podolsky, 1969). In Fig. 2 *A*, the predicted $[Ca^{2+}]_{free}$ profile in a smooth muscle cell without any barriers to diffusion and with an intracellular diffusion coefficient of 4×10^{-6} cm^2/s is shown as a function of time. It can be seen that, even without an intracellular barrier, a substantial gradient of Ca^{2+} developed and persisted for more than 100 ms in the model cell after the start of Ca^{2+} influx through the surface membrane. A maximum $[Ca^{2+}]_{free}$ of 1.13 μM was reached just inside the plasma membrane in the cell 50 ms after the simulation started. During the 100 ms time period modeled, the $[Ca^{2+}]_{free}$ in the cell halfway between the center of the cell and the plasma membrane rose from 150 to 212 nM.

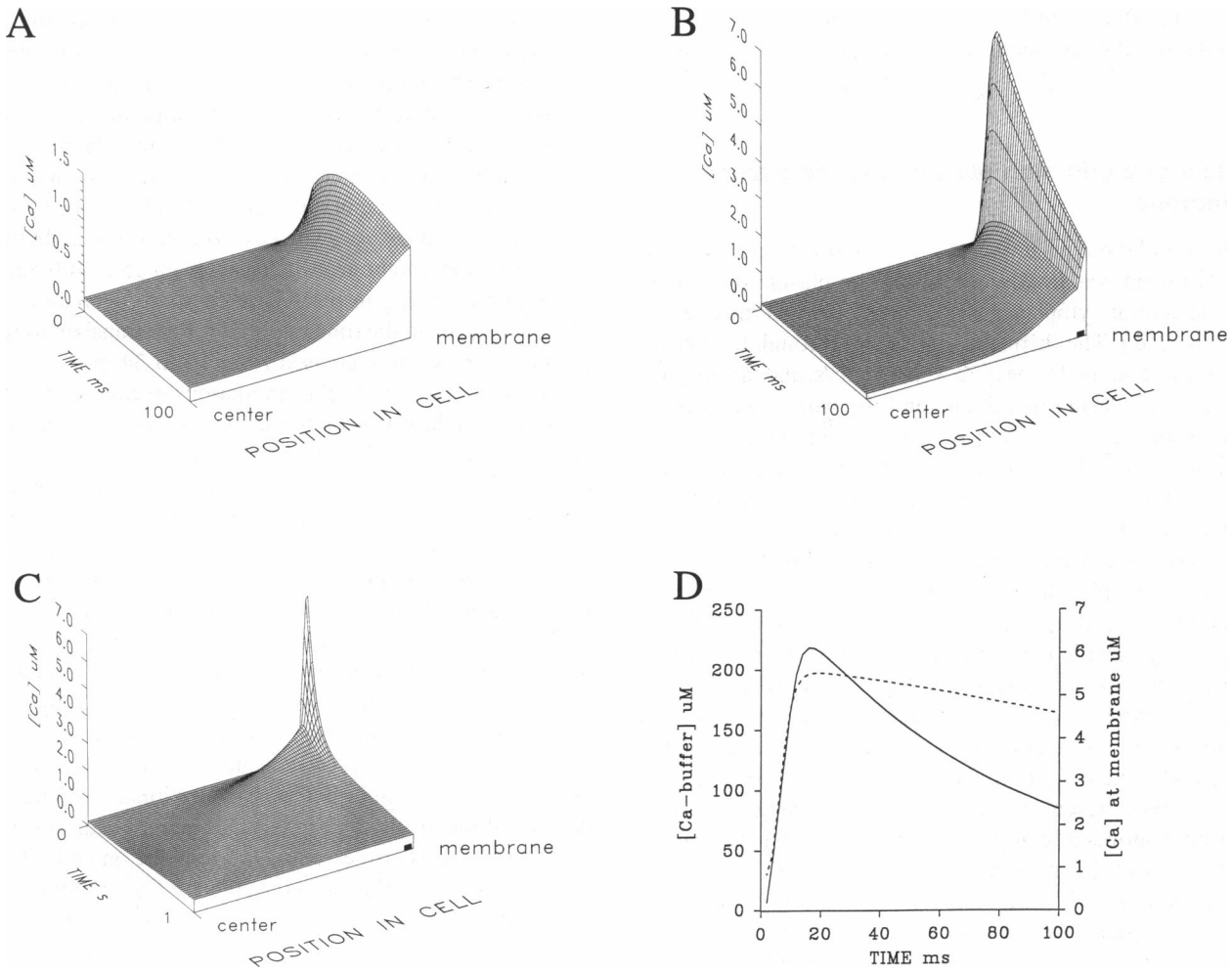

FIGURE 2 (*A*) Time course of radial diffusion without a barrier. $[Ca^{2+}]_{free}$ profiles in the model cell are shown as a function of time with an intracellular diffusion coefficient of 4×10^{-6} cm^2/s (*A*). (*B–D*) Radial diffusion with a barrier. The simulations were similar to those in *A*, but a 100-nm barrier to free diffusion located 25 nm from the plasma membrane was included in the model (the *dark bar* on the radial axis shows the location of the barrier relative to the plasma membrane). The diffusion coefficient through the barrier region was 0.22×10^{-6} cm^2/s; the coefficient in the cytoplasm on either side of the barrier was 2.2×10^{-6} cm^2/s. The $[Ca^{2+}]_{free}$ profiles in the model cell are shown at two time scales: (*B*) 100 ms total time, profiles plotted at 2-ms intervals; (*C*) 1 s total time, profiles plotted at 20-ms intervals. The average $[Ca^{2+}]_{free}$ in the cell was 516 nM after 1 s. (*D*) $[Ca^{2+}]_{free}$ versus time in the restricted space between the plasma membrane and the barrier (——; *right scale*) and Ca^{2+} bound to the Ca^{2+} buffer in this space versus time (- - -; *left scale*). For all of the simulations shown, the cell radius was 3 μm, and the cell was divided into 120 concentric 25-nm annuli.

The recent work of Allbritton et al. (1992) indicates that the diffusion coefficient for Ca^{2+} in cytosolic extracts in which intracellular Ca^{2+} buffers are saturated is approximately 2.2×10^{-6} cm^2/s; roughly one-half the value used in the previous simulation (4×10^{-6} cm^2/s). With a diffusion coefficient of 2.2×10^{-6} cm^2/s, a maximum $[Ca^{2+}]_{free}$ of 1.55 μM was reached near the plasma membrane in the model cell 48 ms after Ca^{2+} influx began, and the $[Ca^{2+}]_{free}$ halfway between the plasma membrane and the center of the cell rose from 150 to 167 nM during a 100 ms time period. Thus, as expected, the lower diffusion coefficient resulted in a steeper Ca^{2+} gradient near the plasma membrane and slower movement of Ca^{2+} into the interior of the cell. The simulations with both diffusion coefficients indicate, however, that the $[Ca^{2+}]_{free}$ near the plasma membrane of a smooth muscle cell is likely to get quite high (1–2 μM) after extracelluar Ca^{2+} influx even in the absence of structural barriers to free diffusion in the cytoplasm. The results further suggest that Ca^{2+}-dependent signal transduction processes are activated near the plasma membrane of a cell before other such processes are effected in the bulk of the cytoplasm.

In the simulations that follow, a cytoplasmic diffusion coefficient of 2.2×10^{-6} cm^2/s was used.

Effects of a diffusion barrier near the plasma membrane

In the simulations in Fig. 2 *B–D*, a 0.1 μm thick barrier to free diffusion was imposed between the plasma membrane and the central cytoplasm of the model smooth muscle cell (see Fig. 1 *B*). The diffusion coefficient through the barrier region was assumed to be 0.22×10^{-6} cm^2/s, and the distance between the plasma membrane and the barrier was varied. With the barrier 25 nm from the plasma membrane, $[Ca^{2+}]_{free}$ in the restricted diffusion space between the plasma membrane and the barrier reached a maximum of 6.1 μM, 16 ms after extracellular Ca^{2+} influx began. The $[Ca^{2+}]_{free}$ in the restricted space then decreased as influx declined, Ca^{2+} binding to the cytoplasmic Ca^{2+} buffer occurred, and Ca^{2+} diffused into the central cytoplasm of the cell. Fig. 2 *B* shows the $[Ca^{2+}]_{free}$ profile in the model cell during the first 100 ms after the start of Ca^{2+} influx, and Fig. 2 *C* shows the profile during the first 1 s. As can be seen in Fig. 2 *C*, although a substantial Ca^{2+} gradient developed in the restricted space under the conditions of the simulation, the very high $[Ca^{2+}]_{free}$ was present for only 100–200 ms, roughly as long as influx continued (compare Figs. 1 *A* and 2 *B*). The rate at which the $[Ca^{2+}]_{free}$ near the membrane declined after reaching a maximum value indicates that, once influx slowed, free Ca^{2+} was rapidly removed from the restricted space. There were three mechanisms in the model that could account for this: (1) extrusion of Ca^{2+} through the plasma membrane; (2) binding of Ca^{2+} to the Ca^{2+} buffer in the restricted space; (3) diffusion of Ca^{2+} through the barrier region into the central cytoplasm of the cell. The rate of Ca^{2+} extrusion (based on estimates of the maximum velocity of the plasma membrane Ca^{2+} pump and the likely contribution of Na^+/Ca^{2+} exchange; see Materials and Methods) was too slow to account for the rate of the decline. The Ca^{2+} transient near the membrane obtained when Ca^{2+} extrusion was not included in the model was virtually identical to the transient obtained when it was included. If the rate at which Ca^{2+} binding to the buffer occurred was slow relative to the rate of Ca^{2+} influx, the $[Ca^{2+}]_{free}$ in the restricted space would decline after influx started to decrease as Ca^{2+} continued to bind to the buffer. Fig. 2 *D* compares the free Ca^{2+} transient in the restricted space for the simulation with the time course of Ca^{2+} binding to the buffer in the space. As can be seen, binding to the buffer was rapid enough to keep up with influx, and additional binding did not occur after the peak of the Ca^{2+} transient was reached. Thus, diffusion of Ca^{2+} out of the restricted space was the primary reason for the rapid decline of the Ca^{2+} transient. The relatively slow unloading of the buffer (Fig. 2 *D*) tended to keep Ca^{2+} in the restricted space. These results indicate that the diffusional properties of a restricted space and the extent of the space would be important determinants of how long a signal persisted in a space once Ca^{2+} influx declined. A low diffusion coefficient in this space or an extended barrier region would favor the confinement of Ca^{2+} in the space and the persistence of transient signals. The buffer in the space would retain Ca^{2+} and, as will be discussed later, might serve as a temporary Ca^{2+} store.

When the distance between the plasma membrane and the diffusion barrier was increased in the model, the maximum $[Ca^{2+}]_{free}$ near the membrane decreased and the time required to reach this maximum increased. As the distance between the plasma membrane was increased from 25 to 100 nm, the maximum $[Ca^{2+}]_{free}$ in the restricted space decreased from 6.1 to 4.9 μM and the time required for the transient to reach its maximum value increased from 16 to 34 ms.

Although, in some of the simulations to follow, it will be assumed that the diffusion barrier was imposed by the physical presence of the SR near the plasma membrane, the work described to this point did not include SR Ca^{2+} uptake or release and, thus, the predicted high Ca^{2+} concentrations could develop anywhere in a cell where an intracellular structure is in close apposition to the plasma membrane. High Ca^{2+} concentrations such as those predicted by the model during Ca^{2+} transients could, in living smooth muscle cells, locally turn on Ca^{2+}-dependent processes near the membrane before the $[Ca^{2+}]$ in the bulk of the cytoplasm changed significantly. The fact that the local Ca^{2+} signal did not persist in the model cell, however, indicates that, in considering this possibility, it is important to have estimates of the time courses of the local Ca^{2+} signals that might occur in smooth muscle cells. It is also essential to know the on and off rates and not just the equilibrium constants for Ca^{2+} binding to the intracellular effector proteins involved to determine whether such signaling is physiologically relevant.

Coupling between Ca^{2+} influx and SR Ca^{2+} release in a restricted diffusion space

To examine the effects of diffusion barriers on the coupling between Ca^{2+} influx through the surface membrane and Ca^{2+} release from the SR, Ca^{2+} release sites were incorporated into

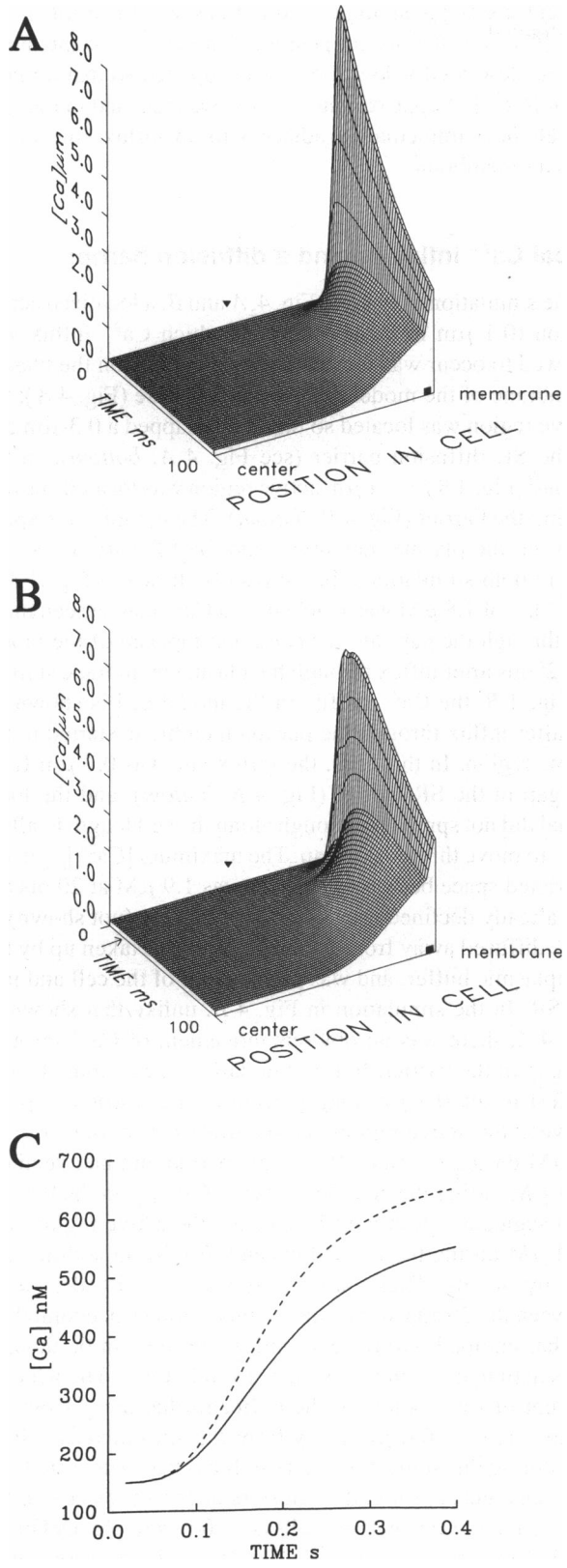

FIGURE 3 Effect of a diffusion barrier on Ca^{2+}-induced Ca^{2+} release from the SR. (*A*, *B*) $[Ca^{2+}]_{free}$ profiles versus time in the model cell with a 100-nm barrier to free diffusion located 25 nm from the plasma membrane (*dark bar* on radial axis as in Fig. 2). (*A*) SR Ca^{2+} release sites were located on the plasma membrane side of the barrier and released Ca^{2+} when the $[Ca^{2+}]_{free}$ in the restricted space between the plasma membrane and the barrier reached 1 μM. (*B*) SR Ca^{2+} release sites were located on the cytoplasmic side of the barrier. Release was triggered when the $[Ca^{2+}]_{free}$ at the sites reached 1 μM. The SR release is apparent in *B* starting at approximately 20 ms (*arrow* on time axis). Other details are given in the text. (*C*) $[Ca^{2+}]_{free}$ in the central cytoplasm of the model cell as a function of time for the two simulations. Cytoplasmic $[Ca^{2+}]_{free}$ was monitored at a point midway between the cell membrane and the center of the cell (*darts* in *A* and *B*). Solid line in *C*: cytoplasmic $[Ca^{2+}]_{free}$ versus time for the simulation in *A*. Dashed line in *C*: cytoplasmic $[Ca^{2+}]_{free}$ versus time for the simulation in *B*.

the model on either the cytoplasmic or the membrane side of the barrier. The cytoplasmic space between the plasma membrane and the SR was set at 25 nm. As in previous work (see Materials and Methods and Kargacin and Fay, 1991), Ca^{2+}-induced Ca^{2+} release from the SR was assumed to occur when the $[Ca^{2+}]_{free}$ at the release sites reached a preset level ([switch]). Even with a [switch] of 1 μM (see Iino 1989), when the release sites faced the plasma membrane, Ca^{2+} release from the SR was triggered very rapidly (release from the SR started 4 ms after influx began). In the results shown in Fig. 3 *A*, a maximum $[Ca^{2+}]_{free}$ of 8.3 μM was reached in the restricted space in the model cell 14 ms after influx began. A situation such as this in a smooth cell would facilitate a very rapid coupling of Ca^{2+} influx to SR release and might compensate somewhat for the low diffusion coefficient for buffered Ca^{2+} in the cell cytoplasm relative to the diffusion coefficients of other second messengers such as IP_3 (see Allbritton et al., 1992). However, the Ca^{2+} released into a restricted diffusion space would be hindered from reaching the bulk of the cytoplasm by the physical presence of the barrier imposed by the SR itself. When the SR Ca^{2+} release sites in the model cell were located on the cytoplasmic side of the diffusion barrier, it took 20 ms for SR Ca^{2+} release to occur after the start of Ca^{2+} influx. The maximum $[Ca^{2+}]_{free}$ that developed in the restricted space in Fig. 3 *B* was lower (6.1 μM) than that seen in Fig. 3 *A*. In this case, SR release was not as rapidly coupled to influx, but Ca^{2+} moved into the central cytoplasm of the cell more rapidly than in the previous simulation. When Ca^{2+} was released into the restricted space, the $[Ca^{2+}]_{free}$ in the central cytoplasm of the model cell (halfway between the cell center and the surface membrane) was 544 nM after 400 ms; when Ca^{2+} was released on the cytoplasmic side of the SR, the concentration at this same time point was 644 nM although, in the latter case, release of Ca^{2+} from the SR took 16 ms longer to start. Plots of $[Ca^{2+}]_{free}$ versus time in the central cytoplasm of the model cell for the two simulations are shown in Fig. 3 *C*.

In previous work with the diffusion models (Kargacin and Fay, 1991), removal of Ca^{2+} from the cytoplasm by the SR Ca^{2+} pumps and extrusion of Ca^{2+} through the plasma membrane were predicted to have little influence on cellular $[Ca^{2+}]$ during the early stages (the first 100 ms) of a transient Ca^{2+} signal. These processes occur on a longer time scale, and the gradients that developed in the model cell near intracellular Ca^{2+} uptake and plasma membrane extrusion sites were much smaller than those seen during Ca^{2+} influx and SR Ca^{2+} release and were apparent in the results only after Ca^{2+} had diffused throughout the cytoplasm. This was also true for the simulations described here. In simulations in

which Ca^{2+}-induced Ca^{2+} release by the SR was allowed to occur into a restricted space (as in Fig. 3 *A*), the inclusion of an SR Ca^{2+} pump on the plasma membrane side of the SR did not noticeably alter the shape, magnitude, or time course of the Ca^{2+} transient in the restricted space over a time period of 100 ms. With the SR pump included in the model, a maximum $[Ca^{2+}]_{free}$ of 8.32 μM was reached in the restricted space after 14 ms; in the absence of the pump a maximum $[Ca^{2+}]_{free}$ of 8.34 μM was reached after 14 ms. There was also little difference in the SR Ca^{2+} content (assuming an initial SR $[Ca^{2+}]_{free}$ of 1.5 mM; see Kargacin et al., 1988) because the Ca^{2+} release process in the SR essentially overwhelmed uptake during the early phases of the transient. It will be shown below that, when localized, low concentrations of Ca^{2+} were allowed to enter a restricted space, and the SR Ca^{2+} content could be increased without SR release.

Simulations with the two-dimensional model

The simulations with the one-dimensional model described thus far provide information about the $[Ca^{2+}]_{free}$ profile along the radius of a cylindrical cell that might be expected if movement of Ca^{2+} into the central cytoplasm of the cell was slowed by the presence of diffusion barriers. An assumption inherent in the model is that Ca^{2+} influx occurs over the entire cell surface and that the radial concentration profile seen in one cross section of the cell would be the same in other cross sections as one moved along the length of the cell. To study the Ca^{2+} signals that might arise as the result of localized Ca^{2+} influx into a smooth muscle cell, two-dimensional models were also developed. As described in Materials and Methods, the black bars in the two-dimensional model in Fig. 1 *C* represent a diffusion barrier, and the open space between the bars represents a gap in the barrier through which free diffusion of Ca^{2+} into the cytoplasm could occur. In the following simulations, Ca^{2+} influx through the plasma membrane was localized to different sites (active regions) along the membrane. The position of the active region, its size, and its position relative to the gap in the diffusion barrier were varied.

As discussed by Hille (1992), a density of open Ca^{2+} channels of approximately $10/\mu m^2$ would be required to account for the macroscopic Ca^{2+} current measured in a typical cell assuming a physiological single channel current of 0.1 pA (see Hille, 1992; Gollasch et al., 1992). Thus, at the 100 nm spatial resolution of the two-dimensional model, assuming a uniform channel density of $10/\mu m^2$, one would expect at most a peak current of 0.1 pA passing through a single Ca^{2+} channel to enter a 100 nm $\times$ 100 nm spatial element (the possibility that Ca^{2+} channels are clustered at certain places in the plasma membrane will be discussed below). Stern (1992) modeled the Ca^{2+} concentration profile opposite a single channel assuming a 1 pA current through the channel. For such a channel, the Stern model predicted a $[Ca^{2+}]$ of approximately 20 μM at a position 50 nm (equivalent to the center of a length and radial element in the present model) from the plasma membrane. If one uses a simple linear scaling to scale down the prediction of Stern's model, a 0.1 pA current under physiological conditions would result in a 2 μM $[Ca^{2+}]$ at the 50 nm position. Therefore, for the simulations described below, Eq. 7 was adjusted so that a maximum $[Ca^{2+}]$ of approximately 2 μM was reached in the spatial element immediately adjacent to an influx site on the plasma membrane.

Local Ca^{2+} influx behind a diffusion barrier

In the simulations shown in Fig. 4, *A* and *B*, a localized active region (0.1 μm in length) through which Ca^{2+} influx was allowed to occur was located at two positions on the plasma membrane of the model cell. In the first case (Fig. 4 *A*), the active region was located so that it overlapped a 0.3-μm gap in the SR diffusion barrier (see Fig. 4 *A*, *bottom*); in the second (Fig. 4 *B*), a 0.1 μm active region was located entirely behind the barrier (Fig. 4 *B*, *bottom*). The cytoplasmic space between the plasma membrane and the SR barrier was 0.1 μm in both simulations. In the results shown in Fig. 4 *A*, a $[Ca^{2+}]_{free}$ of 1.8 μM was reached, and Ca^{2+} can be seen moving through the gap into the central cytoplasm of the model cell 20 ms after influx through the plasma membrane started. In Fig. 4 *B*, the Ca^{2+} profile in the model cell is shown 20 ms after influx through the plasma membrane started in the active region. In this case, the influx site was 0.7 μm from the gap in the SR barrier (Fig. 4 *B*, *bottom*), and the local signal did not spread far enough along the cell length to allow Ca^{2+} to move through the gap. The maximum $[Ca^{2+}]_{free}$ in the restricted space behind the barrier was 1.9 μM at 20 ms but had already declined to 1.40 μM after 40 ms (not shown) as Ca^{2+} diffused away from the influx site, was taken up by the cytoplasmic buffer, and was pumped out of the cell and into the SR. In the simulation in Fig. 4 *B*, unlike that shown in Fig. 4 *A*, there was no obvious movement of Ca^{2+} through the gap in the barrier. In this simulation, the average [Ca^{2+}-buffer] in the 0.4 μm long portion of the restricted space, between the active region and the diffusion barrier, rose by 85 μM during the first 20 ms time period and had declined by 7 μM during the next 20 ms. The $[Ca^{2+}]_{free}$ in the 0.4 μm long segment within the SR opposite the active region rose by 4 μM during the first 20 ms and rose by an additional 4 μM by 40 ms. Thus, half of the Ca^{2+} lost by the buffer between the 20 and 40 ms time points could be accounted for by that pumped into the SR, and the buffer can be thought of as acting as a temporary store for this Ca^{2+}. The average amount of Ca^{2+} bound to the buffer further away from the influx site (0.2–0.6 μm away from the site) increased by 3 μM during this same time interval. It has been suggested that Ca^{2+} channels are found in clusters at certain places on the plasma membrane of some cells (see, for example, DeFelice, 1993; Risso and DeFelice, 1993). If this is the case, much higher local Ca^{2+} currents would occur at such locations. When the Ca^{2+} permeability of the plasma membrane in the model cell was increased by a factor of 10 over that used in the simulations described above (10-channel cluster), the $[Ca^{2+}]_{free}$ in the restricted space for the simulation in Fig. 4 *B* was 18.1 μM at 20 ms and 12.3 μM at 40 ms. Note: a high $[Ca^{2+}]_{free}$ such as this would also be seen at the SR membrane

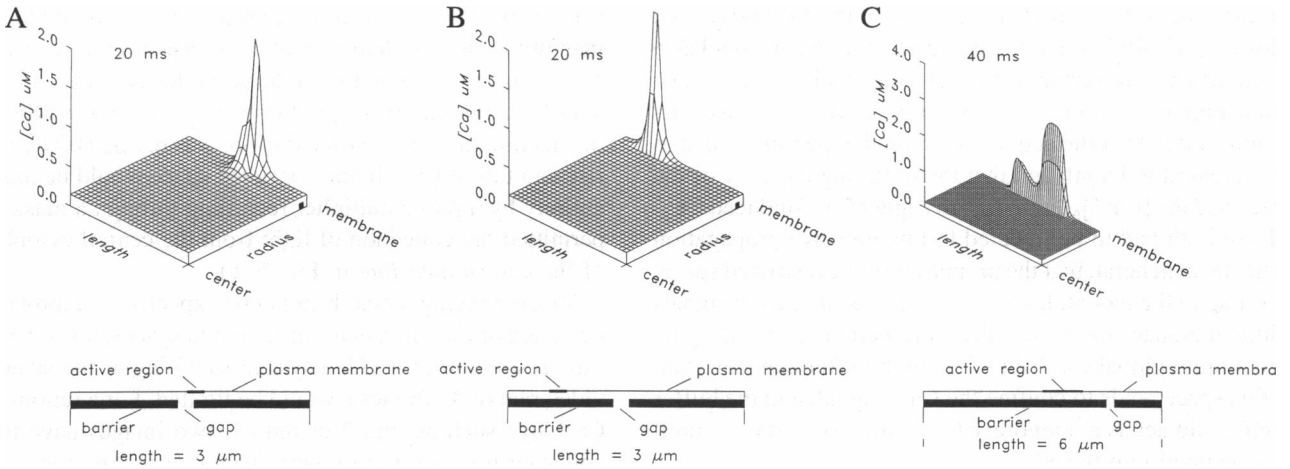

FIGURE 4 Ca^{2+} diffusion in two dimensions. (*A*, *top*) The $[Ca^{2+}]_{free}$ in the model cell is shown 20 ms after a localized influx of Ca^{2+} through the plasma membrane began. (*A*, *bottom*) Schematic of the cell near the plasma membrane showing the relationship between the influx site (active region), an intracellular diffusion barrier (*dark bars*) and a gap in the barrier. In this case, the active region overlapped the location of the gap in the barrier and Ca^{2+} can be seen in the central cytoplasm of the cell in the region of the gap. (*B*, *top*) The $[Ca^{2+}]_{free}$ in the model cell is shown 20 ms after Ca^{2+} influx through the active region started. In this case, the active region of the membrane was located entirely behind the diffusion barrier (*B*, *bottom*) and Ca^{2+} did not reach the gap or move into the central cytoplasm. For the simulations in *A* and *B*, the cell was divided into 30 100-nm concentric annuli and 30 100-nm length elements. The diffusion barrier was 100 nm thick and was located 100 nm from the plasma membrane. (*C*) Generation of a Ca^{2+} wave in the restricted space between the SR and the plasma membrane. For this simulation, the active region was 1 μm long and was located entirely behind the diffusion barrier (*C*, *bottom*). The cell was divided into 30 100-nm concentric annuli and 60 100-nm length elements. Other details of the simulation are the same as those for the simulation in *A* and *B* or are described in the text. The $[Ca^{2+}]_{free}$ profile in the cell is shown 40 ms after Ca^{2+} influx through the active region started. Note the Ca^{2+} wave on the left side of the active region propagating toward the upper left of the figure. For the simulations shown in *A–C*, the diffusion coefficient through the barrier region was 0.22×10^{-6} cm^2/s; the coefficient in the cytoplasm on either side of the barrier and through the gap was 2.2×10^{-6} cm^2/s.

near a single Ca^{2+} channel if the distance between the SR and the plasma membrane was less than the 0.1 μm separation that was used in the present simulations. In the 10-channel simulation, the average $[Ca^{2+}]$ in the 0.4 μm length of SR opposite the influx site increased by 4 μM, and the average [Ca^{2+}-buffer] decreased from 210 to 202 μM during the time interval between 20 and 40 ms. Although the higher Ca^{2+} influx resulted in a higher local $[Ca^{2+}]_{free}$, the Ca^{2+} signal in the model cell remained confined (qualitatively similar to the result shown in Fig. 4 *B*), and no obvious movement of Ca^{2+} through the gap in the barrier was visible.

Small Ca^{2+} influxes, such as those described above, into a restricted diffusion space between the plasma membrane and the SR in a smooth muscle cell could be a means of loading the SR. This could occur without a corresponding change in $[Ca^{2+}]$ in the central cytoplasm large enough to elicit a contractile response in a cell. Conversely, small amounts of Ca^{2+} released by the SR into a restricted space could be pumped out of a cell as a means of regulating SR Ca^{2+} content without eliciting changes in the central cytoplasmic $[Ca^{2+}]$ or contractile responses. These simulations suggest that localized Ca^{2+} influx behind a diffusion barrier could remain localized and could be used by the cell to regulate enzymes confined to such regions.

Local Ca^{2+} influx, SR Ca^{2+} release, and the propagation of Ca^{2+} waves

In the simulations with the two-dimensional model described above, the SR was allowed to take up Ca^{2+} from the restricted space opposite the active region of the plasma membrane, but SR release was not included in the model. If the Ca^{2+} in the restricted space did trigger SR release, one might expect that the release could become regenerative and initiate a wave of Ca^{2+} release that propagated along the surface membrane in the space. In this way, a confined Ca^{2+} signal, due to a localized influx of Ca^{2+} large enough to trigger SR Ca^{2+} release, might lead to a more global intracellular release of Ca^{2+} and possibly a contractile response. To test this possibility, the diffusion barrier in the two-dimensional model was constructed as in the previous simulations shown in Fig. 4 *B*. In the present case, however, SR release was allowed to occur when the $[Ca^{2+}]_{free}$ in the space reached 1 μM. Although SR Ca^{2+} release into the restricted space was triggered by the Ca^{2+} influx expected from a single Ca^{2+} channel, even when a cluster of 10 channels was incorporated into the model, the Ca^{2+} signal did not propagate along the membrane (not shown but qualitatively similar to the Ca^{2+} signal in Fig. 4 *B*). When the total buffer concentration in the space was reduced from 230 to 115 μM, the active region of the membrane was expanded to 1 μm and the [switch] was lowered to 400 nM; the local Ca^{2+} influx did lead to the formation of a Ca^{2+} pulse or wave that propagated along the cell length in the restricted space in one direction (toward the *upper left* in Fig. 4 *C*). However a 0.2-μm gap in the SR barrier (located 0.4 μm away from the influx site; see schematic in Fig. 4 *C*) effectively prevented a wave from moving in the other direction (toward the *lower right*) in the cell. These results indicate that Ca^{2+} waves dependent on Ca^{2+}-induced Ca^{2+} release could propagate along the cell length through a restricted space but also indicate that the size of the space and its Ca^{2+} buffering capacity exert critical influences

on this type of Ca^{2+} movement. Gaps in the SR barrier that allowed Ca^{2+} diffusion into the central cytoplasm would also be important determinants of the extent to which a Ca^{2+} wave could propagate along the cell length in the restricted diffusion space. That the active region on the membrane had to be increased in length and that the buffering capacity of the space and the $[Ca^{2+}]_{free}$ required to trigger Ca^{2+}-induced Ca^{2+} release both had to be lowered to initiate wave propagation indicate, in general, that the properties of the restricted space, as set up in the model, favor the confinement of local signals within this space rather than the transduction of a local signal into a more global Ca^{2+} signal. A high buffer concentration in this space tends to confine the Ca^{2+} signal, and the buffer itself could act as a temporary Ca^{2+} store to hold Ca^{2+} until it is pumped into the SR.

Predictions for the measurement of intracellular Ca^{2+} in experiments on smooth muscle

At present, many laboratories are actively involved in using fluorescent indicators to measure Ca^{2+} transients in smooth muscle cells. Fluorescence signals are either collected with a photomultiplier from a masked region of a cell or video images of the cell are acquired. To determine how a Ca^{2+} signal in a restricted space might be perceived with a non-imaging method of measurement, the average $[Ca^{2+}]_{free}$ over the entire model cell for the simulation shown in Fig. 2 *B–D* and the average $[Ca^{2+}]_{free}$ in the central cytoplasm of the cell (averaged over the central 4.5 μm of a 6 μm diameter cell) were compared with the Ca^{2+} transient in the restricted space. A photomultiplier recording through a mask that allowed the collection of light from the entire cell, including the area near the plasma membrane, would be expected to produce a signal similar to the average Ca^{2+} curve (*dashed line*) in Fig. 5 *A*. An initial transient peak in $[Ca^{2+}]_{free}$ corresponding to the Ca^{2+} peak in the restricted space is present in this signal. The magnitude and the sharpness of the transient in the restricted space, however, are not reproduced in the average Ca^{2+} signal (the maximum $[Ca^{2+}]$ in the average curve was 680 nM; the maximum in the restricted space was 6.1 μM). The rapid rise and fall of Ca^{2+} in the restricted space would be missed entirely by a photomultiplier recording through a mask that permitted the collection of light from the central cytoplasm of the cell (*dotted line* in Fig. 5 *A*).

Video imaging methods might be expected to improve the detection of Ca^{2+} transients in restricted spaces; however, the time resolution of a video system sampling at the standard video rate of 30 frames/s would be limited. For a ratiometric Ca^{2+} dye such as fura-2 or indo-1, two images have to be collected for each ratio image. This reduces the time resolution to 15 frames/s. Fig. 5 *B* (*solid line*) shows the Ca^{2+} transient in the restricted space (from Fig. 2 *B*) and the transient in the space (*filled circles* and *dashed line*) that would be recorded by a system (with sufficient spatial resolution to record Ca^{2+} in the 25 nm restricted space) that collected light and computed the $[Ca^{2+}]_{free}$ in the space 17 times/s (the concentrations shown by the solid circles in Fig. 5 *B* are the average concentrations in the restricted diffusion space over each sampling period).

In the above discussion, it was assumed that a Ca^{2+} dye would not add additional Ca^{2+} buffering capacity to the model cell (for discussions of the effects of the addition of Ca^{2+} buffers to cells, see Stern, 1992; Blumenfeld et al., 1992). It was also assumed that light could be collected from a single image plane (high z axis resolution). Addition of Ca^{2+} buffer to a living smooth muscle cell would reduce the magnitude of and slow down a transient Ca^{2+} signal. Out of focus light from the area near the membrane of a cell above and below a central plane of focus might actually allow a Ca^{2+} transient near the membrane to be recorded from a

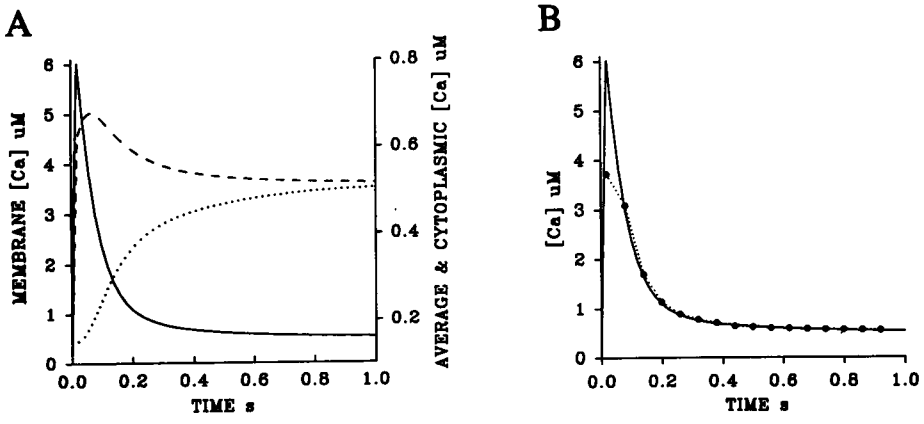

FIGURE 5 Simulated measurements of $[Ca^{2+}]_{free}$. (*A*) $[Ca^{2+}]_{free}$ in the restricted space (——, *left scale*); average $[Ca^{2+}]_{free}$ over the entire model cell (- - -, *right scale*); and average central cytoplasmic $[Ca^{2+}]_{free}$ (···, *right scale*) for the simulation in Fig. 2 *B*. To calculate average $[Ca^{2+}]_{free}$ over the entire model cell, the total free Ca^{2+} in each annulus in the model cell was computed and used to determine the total free Ca^{2+} in the cell. This value was then divided by the cell volume. To calculate the average central cytoplasmic $[Ca^{2+}]_{free}$, the total free Ca^{2+} in each annulus for the first 90 annuli in the cell (central 4.5 μm of the 6 μm diameter cell) was computed and used to determine the total free Ca^{2+} in this region. Total free Ca^{2+} was then divided by the volume of the region. Note: on the right hand scale in *A* average $[Ca^{2+}]$ = average $[Ca^{2+}]_{free}$ across the entire cell; cytoplasmic $[Ca^{2+}]$ = average $[Ca^{2+}]_{free}$ across the central cytoplasm of the model cell. (*B*) $[Ca^{2+}]_{free}$ in the restricted space (——) and the $[Ca^{2+}]_{free}$ (···●···) that would be reported by a measurement in which the $[Ca^{2+}]_{free}$ in the restricted space was averaged over 59 ms time intervals and reported at a rate of 17/s.

measurement of Ca^{2+} in the central cytoplasm of a cell. The results presented above, however, indicate that, in general, such transients would be only poorly resolved experimentally. Until improvements in the temporal and spatial resolution of current experimental techniques for the direct measurement of intracellular Ca^{2+} are made, the most sensitive methods for detecting local Ca^{2+} changes near the plasma membrane in cells are probably those that indirectly do this by monitoring Ca^{2+}-dependent changes in ion channel activity.

SUMMARY

The purpose of this study was to provide a general description of the temporal and spatial characteristics of the Ca^{2+} concentration gradients that might develop in smooth muscle cells after Ca^{2+} influx through the plasma membrane into regions where there are barriers that inhibit the free movement of Ca^{2+} into the central cytoplasm. The parameters describing the Ca^{2+} regulatory mechanisms that were built into the model were based as much as possible on those derived experimentally and were assumed to be the same throughout the cell. Results of the simulations indicate the following.

- Very high Ca^{2+} concentrations and steep gradients can develop in cells during transient Ca^{2+} signals, especially where free diffusion into the cytoplasm is restricted by the presence of physical barriers.
- The Ca^{2+} gradients and concentrations that accompany the influx of Ca^{2+} into the cell from the extracelluar space might themselves be important elements of a Ca^{2+} signal and serve to couple influx to intracellular Ca^{2+} release. These local signals might also activate Ca^{2+}-dependent signal transduction pathways near the plasma membrane before triggering cell contraction. Local Ca^{2+} influx or release into a restricted space might also occur and raise the $[Ca^{2+}]$ in the space without significantly changing the $[Ca^{2+}]$ of the central cytoplasm of the cell.
- These local Ca^{2+} signals might serve to regulate intracellular Ca^{2+} stores or might provide a means by which the same second messenger (e.g., Ca^{2+}) could activate different signal transduction pathways in response to different stimuli.

The results as a whole indicate that it is important to consider intracellular second messenger signals not only in terms of their temporal characteristics but also in terms of how these signals might be spatially distributed in a cell.

The author wishes to thank Drs. Gisele Scott-Woo, Michael P. Walsh, and Margaret E. Kargacin for their critical comments on the manuscript. The author is an Alberta Heritage Foundation Scholar.

This work was supported by National Institutes of Health grant AR39678 and the Heart and Stroke Foundation of Alberta.

REFERENCES

Allbritton, N. L., T. Meyer, and L. Stryer. 1992. Range of messenger action of calcium ion and inositol 1,4,5-trisphosphate. *Science.* 258:1812–1815.

Backx, P. H., P. P de Tombe, J. H. K. Van Deen, B. J. M. Mulder, and H. E. D. J. ter Keurs. 1989. A model of propagating calcium-induced calcium release mediated by calcium diffusion. *J. Gen. Physiol.* 93: 963–977.

Bading, H., D. D. Ginty, and M. E. Greenberg. 1993. Regulation of gene expression in hippocampal neurons by distinct calcium signaling pathways. *Science.* 260:181–186.

Becker, P. L., J. J. Singer, J. V. Walsh, Jr., and F. S. Fay. 1989. Regulation of calcium concentration in voltage-clamped smooth muscle cells. *Science.* 244:211–214.

Benham, C. D., and T. B. Bolton. 1986. Spontaneous transient outward currents in single visceral and vascular smooth muscle cells of the rabbit. *J. Physiol.* 381:385–406.

Blaustein, M. P., R. DiPolo, and J. P. Reeves, editors. 1991. Sodium-Calcium Exchange: Proceedings of the Second International Conference. The New York Academy of Sciences, New York. 482–575.

Blumenfeld, H., L. Zablow, and B. Sabatini. 1992. Evaluation of cellular mechanisms for modulation of calcium transients using a mathematical model of fura-2 Ca^{2+} imaging in *Aplysia* sensory neurons. *Biophys. J.* 63:1146–1184.

Bond, M., H. Shuman, A. P. Somlyo, and A. V. Somlyo. 1984. Total cytoplasmic calcium in relaxed and maximally contracted rabbit portal vein smooth muscle. *J. Physiol.* 357:185–201.

Cannell, M. B., and D. G. Allen. 1984. Model of calcium movements during activation in the sarcomere of frog skeletal muscle. *Biophys. J.* 45: 913–925.

Carafoli, E. 1987. Intracellular calcium homeostasis. *Annu. Rev. Biochem.* 56:395–433.

Cooney, R. A., T. W. Honeyman, and C. R. Scheid. 1991. Contriburion of Na^+-dependent and ATP-dependent Ca^{2+} transport to smooth muscle calcium homeostasis. *In* Sodium-Calcium Exchange: Proceedings of the Second International Conference. M. P. Blaustein, R. DiPolo, and J. P. Reeves, editors. The New York Academy of Sciences, New York. 558–560.

Crank, J. 1975. The Mathematics of Diffusion. Oxford University Press, New York. 414 pp.

DeFelice, L. J. 1993. Molecular and biophysical view of the Ca channel: a hypothesis regarding oligomeric structure, channel clustering and macroscopic current. *J. Membr. Biol.* 133:191–202.

Désilets, M., S. P. Driska, and C. M. Baumgarten. 1989. Current fluctuations and oscillations in smooth muscle cells from hog carotid artery: role of the sarcoplasmic reticulum. *Circ. Res.* 65:708–722.

Devine, C. E., A. V. Somlyo, and A. P. Somlyo. 1972. Sarcoplasmic reticulum and excitation-contraction coupling in mammalian smooth muscles. *J. Cell Biol.* 52:690–718.

Fleischer, S., and M. Inui. 1989. Biochemistry and biophysics of excitation-contraction coupling. *Annu. Rev. Biophys. Biophys. Chem.* 18:333–364.

Gabella, G. 1983. Structure of smooth muscles. *In* Smooth Muscle: an Assessment of Current Knowledge. E. Bulbring, A. F. Brading, A. W. Jones, and T. Tomita, editors. University of Texas Press, Austin, TX. 1–46.

Gollasch, M., J. Hescheler, J. M. Quale, J. P. Patlak, and M. T. Nelson. 1992. Single calcium channel currents of arterial smooth muscle at physiological calcium concentrations. *Am. J. Physiol.* 263:C948–C952.

Hille, B. 1992. Ionic Channels of Excitable Membranes. Sinauer Associates Inc., Sutherland, MA. 607 pp.

Hume, J. R., and N. Leblanc. 1989. Macroscopic K^+ currents in single smooth muscle cells of the rabbit portal vein. *J. Physiol.* 413:49–73.

Iino, M. 1989. Calcium-induced calcium release mechanism in guinea pig taenia caeci. *J. Gen. Physiol.* 94:363–383.

Kargacin, G., and F. S. Fay. 1991. Ca^{2+} movement in smooth muscle cells studied with one- and two-dimensional diffusion models. *Biophys. J.* 60: 1088–1100.

Kargacin, M. E., C. R. Scheid, and T. W. Honeyman. 1988. Continuous monitoring of Ca^{2+} uptake in membrane vesicles with fura-2. *Am. J. Physiol.* 245:C694–C698.

Kushmerick, M. J., and R. J. Podolsky. 1969. Ionic mobility in muscle cells. *Science.* 166:1297–1298.

Leblanc, N., and J. R. Hume. 1990. Sodium current-induced release of calcium from cardiac sarcoplasmic reticulum. *Science.* 248:372–376.

Lederer, W. J., E. Niggli, and R. W. Hadley. 1990. Sodium-calcium exchange in excitable cells: fuzzy space. *Science.* 248:283.

Lucchesi, P. A., R. A. Cooney, C. Mangsen-Baker, T. W. Honeyman, and C. R. Scheid. 1988. Assessment of transport capacity of plasmalemmal Ca^{2+} pump in smooth muscle. *Am. J. Physiol.* 255:C226–C236.

Ohya, Y., K. Kitamura, and H. Kuriyama. 1987. Cellular calcium regulates outward currents in rabbit smooth muscle cell. *Am. J. Physiol.* 252: C401–C410.

Risso, S., and L. J. DeFelice. 1993. Ca channel kinetics during the spontaneous heart beat in embryonic chick ventricle cells. *Biophys. J.* 65: 1006–1018.

Robertson, S. P., J. D. Johnson, and J. D. Potter. 1981. The time-course of Ca^{2+} exchange with calmodulin, troponin, parvalbumin, and myosin in response to transient increases in Ca^{2+}. *Biophys. J.* 34:559–569.

Smith, S. J., and G. J. Augustine. 1988. Calcium ions, active zones and synaptic transmitter release. *TINS.* 11:458–464.

Somlyo, A. V. 1980. Ultrastructure of vascular smooth muscle. *In* The Handbook of Physiology: The Cardiovascular System. Vol. 2. Vascular Smooth Muscle. D. F. Bohr, A. P. Somlyo, and H. V. Sparks, Jr., editors. American Physiological Society, Bethesda, MD. 33–67.

Somlyo, A. V., and C. Franzini-Armstrong. 1985. New views of smooth muscle structure using freezing, deep-etching and rotary shadowing. *Experimentia.* 41:841–856.

Stehno-Bittel, L., and M. Sturek. 1992. Spontaneous sarcoplasmic reticulum calcium release and extrusion from bovine, not porcine, coronary artery smooth muscle. *J. Physiol.* 451:49–78.

Stern, M. D. 1992. Buffering of calcium in the vicinity of a channel pore. *Cell Calcium.* 13:183–192.

Sturek, M., K. Kunda, and Q. Hu. 1992. Sarcoplasmic reticulum buffering of myoplasmic calcium in bovine coronary artery smooth muscle. *J. Physiol.* 451:25–48.

van Breemen, C., and K. Saida. 1989. Cellular mechanisms regulating $[Ca^{2+}]_i$ smooth muscle. *Annu. Rev. Physiol.* 51:315–329.